

PAPER • OPEN ACCESS

## Wind-wave directional effects on fatigue of bottom-fixed offshore wind turbine

To cite this article: S H Sørum *et al* 2019 *J. Phys.: Conf. Ser.* **1356** 012011

View the [article online](#) for updates and enhancements.



**IOP | ebooks™**

Bringing you innovative digital publishing with leading voices to create your essential collection of books in STEM research.

Start exploring the collection - download the first chapter of every title for free.

# Wind-wave directional effects on fatigue of bottom-fixed offshore wind turbine

S H Sørum<sup>1</sup>, J R Krokstad<sup>2</sup>, J Amdahl<sup>1</sup>

<sup>1</sup> Centre for Autonomous Marine Operations and Systems, Department of Marine Technology, Norwegian University of Science and Technology, NO-7491 Trondheim

<sup>2</sup> Department of Marine Technology, Norwegian University of Science and Technology, NO-7491 Trondheim

E-mail: [stian.h.sorum@ntnu.no](mailto:stian.h.sorum@ntnu.no)

## Abstract.

The current trend for offshore wind energy is that larger turbines are placed on monopile foundations at increasing water depth. This requires larger foundations, increasing the importance of hydrodynamic loading. It is well established that wave loads perpendicular to the wind direction are important for the fatigue damage in monopile foundations. However, this is normally only taken into account considering wind-wave misalignment. In this paper, the effect of assuming short-crested waves in design calculations is considered. The lifetime fatigue damage may increase significantly for hydrodynamically sensitive support structures when modelling the waves as short-crested rather than long-crested. For the turbines in this paper, the fatigue damage increased with up to 80 %. At the same time, the changes in fatigue damage were small for support structures that are less hydrodynamically sensitive. The work performed in this paper shows that the typical design assumption of long-crested waves may be both conservative and non-conservative. This fact is important to be aware of when designing support structures for offshore wind turbines.

## 1. Introduction

Offshore wind turbines (OWTs) are subject to several sources of dynamic loading, including wind and wave loads. With increasingly large turbines being installed[1], the aerodynamic loads increase. Larger loads, in turn, lead to increased capacity requirements for the support structure. In Europe, monopiles are the dominating foundation type, making up 66 % of all installations in 2018[1]. Increasing the structural capacity of these foundations often leads to larger dimensions, which in turn increases the wave loading. Further, new turbines are typically installed in deeper water, with 27 m being the average for 2018[1]. This serves to increase the importance of wave loads relative to wind loads.

Fatigue damage is typically determining the final dimensions of monopile foundations[2]. Wave-induced responses contribute to this fatigue damage, especially when wind and waves are misaligned[3]. For wind-wave misalignment, the lack of aerodynamic damping in the crosswind direction gives large responses even for moderate excitation. Fischer et al.[3] have previously shown the importance of including misalignment in design calculations for a 5 MW turbine, and the sensitivity of the transverse response to damping levels was demonstrated by Koukoura et al.[4]. Kim and Natarajan[5] showed the importance of deeper water, demonstrating increased



importance of misalignment conditions when the water depth was raised from 25 to 35 meters. The influence of soil modelling was also shown, giving increased fatigue damage for softer soil. Smilden et al.[6] showed that misalignment angles up to  $45^\circ$  contribute significantly to the fatigue damage of a large diameter monopile. Design standards such as [7] also require that wind-wave misalignment is included in design calculations.

Common for the papers [3]-[6] is that the misalignment between wind and *long-crested* waves is considered. However, wind-wave misalignment may also occur from *short-crested* waves. For a structure with uniform properties, Vugts[8] showed that it is conservative to assume long-crested waves. This conclusion cannot be generalized for OWTs, due to the presence of aerodynamic damping only in-line with the wind. In a short-term perspective, the fatigue damage from short-crested waves can be both larger or smaller than the fatigue damage from long-crested waves. This will, amongst others, depend on the misalignment between the wind and the mean wave direction, the level of wave spreading and which position on the structure that is considered most critical for fatigue. Few studies exist on the effect of short-crested waves on OWTs, but Trumars, Jonsson and Bergdal[9] investigated this using measurement data from a 500 kW turbine at 6.5 m water depth. Horn, Krokstad and Amdahl[10] investigated several aspects of wave modelling by considering wave excitation and aerodynamic damping. Kim and Natarajan[5] showed that the soil stiffness is important for how wind-wave misalignment influences fatigue damage. As short-crested waves introduce further wind-wave misalignment, it is expected that the soil stiffness will influence also the effect of wave spreading.

This paper contributes to increasing the knowledge about the response of monopile supported OWTs to short-crested waves, and how this differs from the response to long-crested waves. The primary goal is to assess whether the assumption of long-crested waves in design calculations yields conservative estimates of the lifetime fatigue damage in the support structure. Further, the influence of varying sensitivity to wave loading is assessed by using models with different mode shapes. Both the natural period of the first global tower modes and the corresponding mode shapes influence the importance of wave loads. Only changes in the mode shapes are considered here, as OWTs are typically designed with a target natural frequency[11]. The analyses consider three similar monopile foundations in varying soil conditions. The towers are tuned to give the desired natural frequencies. A long-term fatigue analysis is performed for each design, to demonstrate how the different mode shapes affect the fatigue damage in long-crested or short-crested waves.

The paper is organised as follows: Section 2 presents the wave directionality effects considered. In Section 3 the OWT and simulation set-up used in this study is described. Following this, the simulation results are given in Section 4; first for aligned wind and waves to determine the relative importance of wind and wave loads, then for long-crested and short-crested waves including wind-wave misalignment. Finally, the results are discussed in Section 5, and a conclusion is drawn.

## 2. Wave directionality

Wind-wave misalignment may occur from misalignment between the wind direction and the mean wave direction, as well as from wave spreading. Further, wind driven waves and swell waves may behave differently with regards to misalignment. Wind generated waves will typically travel in a direction close to the wind direction, but can have significant wave spreading. Swell waves are generated independent of the local wind conditions, and may have more pronounced misalignment. This will depend on the dominating wind directions and swell directions at each individual site. At the same time, swell waves are mainly long-crested, meaning that all waves travel in the same direction.

The difference between wind waves and swell in terms of misalignment is shown in Figure 1 for the site described in Section 3.3. The figure shows the absolute value of misalignment

for swell waves to the left and for wind waves to the right. It is clear that the misalignment is limited for wind-generated waves, while all misalignment angles occur for the swell waves.

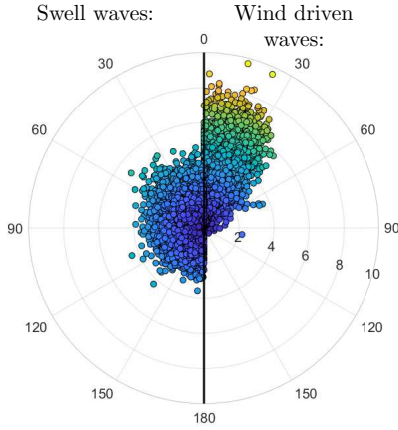


**Figure 1.** Scatter of absolute value of wind-wave misalignment for swell (left) and wind driven waves (right). The radial axis shows  $H_s$  in metres.

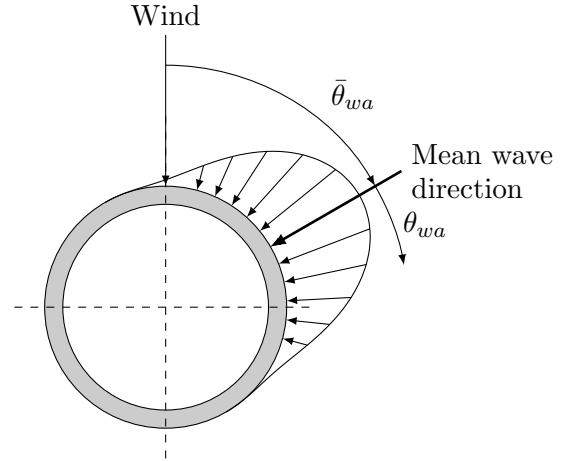


**Figure 2.** Mean wave direction,  $\bar{\theta}_{wa}$ , and direction of wave components,  $\theta_{wa}$ , relative to wind direction

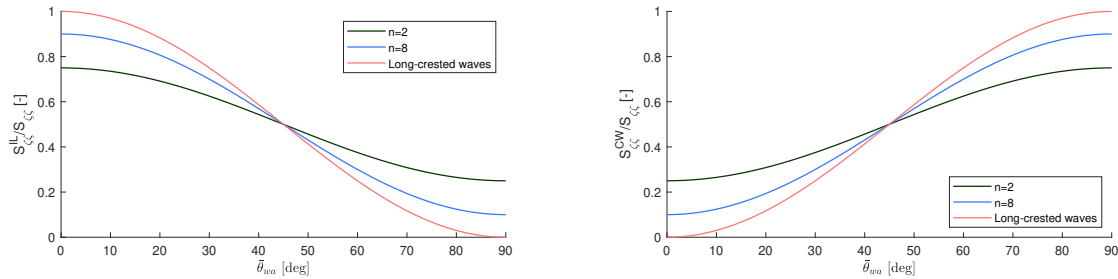


**Figure 3.** Ratio of in-line (left) and crosswind (right) wave spectrum as function of mean misalignment angle.

Several engineering models for wave spreading can be used in the analyses. These include both frequency independent and frequency dependent models. DNV GL[12] recommends modelling short-crested waves by multiplying the unidirectional wave spectrum,  $S_{\zeta\zeta}(\omega)$ , with a directional spreading function  $D(\theta_{wa})$ . The wave spectrum for short-crested waves is then given as

$$S_{\zeta\zeta}(\omega, \theta_{wa}) = S_{\zeta\zeta}(\omega)D(\theta_{wa}) \quad (1)$$

Here,  $\theta_{wa}$  is the angle of each directional component relative to the mean wave direction  $\bar{\theta}_{wa}$  as shown in Figure 2. The formulation for  $D(\theta_{wa})$  used in this paper is

$$D(\theta_{wa}) = \frac{\Gamma(1 + n/2)}{\sqrt{\pi}\Gamma(1/2 + n/2)} \cos^n(\theta_{wa} - \bar{\theta}_{wa}) \quad (2)$$

with  $|\theta_{wa} - \bar{\theta}_{wa}| \leq \pi/2$ [12]. The spreading exponent  $n$  is typically in the range 2-4 for wind waves, while  $n > 7$  is recommended for swell waves.

For OWTs, it is interesting to consider the wave energy travelling in the same direction as the wind and that travelling perpendicular to the wind. The energy distribution will vary with both the mean wave direction and wave spreading. Figure 3 shows the ratio of total wave energy travelling in-line with the wind and in the crosswind direction for different misalignment angles. The figure shows that short-crested waves will increase the crosswind wave energy for misalignment angles up to  $45^\circ$ . For wind driven waves, conditions with less than  $45^\circ$  misalignment can be expected to dominate, and a significant increase in the crosswind response will be seen. At the same time, the aerodynamic loads will contribute to the response in-line with the wind. The reduction in response in the in-line direction will, therefore, be less than the reduction in wave loading.

### 3. Methodology

This paper investigates the effect of wave directionality by performing time-domain simulations. In this section, the simulation models and methodology is presented.

#### 3.1. Model description

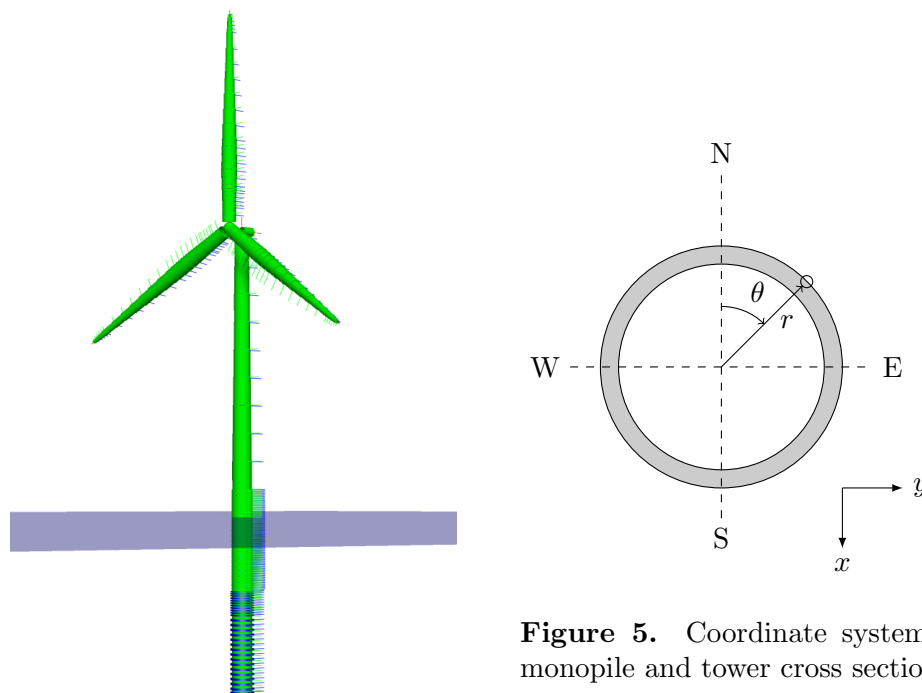


**Figure 4.** Wind turbine model in SIMA

**Figure 5.** Coordinate system of monopile and tower cross section.

The turbine model is based on the DTU 10 MW reference wind turbine [13], and is shown in Figure 4. Compared to the reference turbine, the inner blade foils have been altered and the tower has been stiffened by increasing the wall thickness by 20 %, both as described in [14]. The tower is placed on a monopile foundation with a diameter of 8 m and wall thickness of 0.11 m, standing in 30 m water depth. Below the mudline, the monopile extends for another 42 m. The characteristics of the soil springs are based on the  $p - y$  curves computed in accordance with ISO 19901-4[15] for a location at Dogger Bank.

**Table 1.** Variation in parameters between models, given as fraction of the value for the base model

Parameter	Base model	Soft model	Stiff model
Relative soil stiffness	1	0.65	8
Relative tower wall thickness	1	1.65	0.725

**Table 2.** Natural frequencies of models, in [Hz]

Mode	Base model	Stiff soil	Soft soil
1st fore-aft	0.2069	0.2072	0.2063
2nd fore-aft	1.0522	1.3014	0.9708
1st side-side	0.2063	0.2061	0.2060
2nd side-side	1.0100	1.3665	1.0022

Structural and soil damping is modelled as stiffness proportional Rayleigh damping. To account for soil damping, the damping coefficient is doubled below the mudline. In [16], a review of measured damping levels of monopile OWTs is given, and the damping is found to vary between 1.1 % and 2.8 % of critical damping. A damping level of 1.1 % at the first tower mode was therefore selected to ensure conservative results.

The simulations are carried out in the aero-hydro-servo-elastic computer program SIMA v. 3.2.2, developed by SINTEF Ocean. All structural members are modelled as non-linear beam elements, while soil-structure interaction is modelled by non-linear springs. Hydrodynamic loads are calculated using Morison's equation based on linear wave kinematics evaluated to the mean water level, while aerodynamic loads are calculated with the blade element momentum theory including dynamic inflow, dynamic wake, tip loss and tower shadow effects[17].

### 3.2. Variations to model

In order to analyse the effect of varying sensitivity to wave loads, two additional models were created. The model described in Section 3.1 will hereafter be referred to as the base model. Further, one model with stiffer soil and one model with softer soil were analysed by linear scaling of the p-y curves. These will be referred to as the stiff model and soft model, respectively.

In order to get comparable results and similar environmental loads, the natural period of the 1st global tower mode and the outer diameter of the structures were kept unchanged. Together with the soil stiffness, this left the tower wall thickness as the parameter that could be changed in the models. For the soft model this set a limit to how much the soil stiffness could be reduced while still keeping the natural frequencies at the target values. The stiff model was then altered to give a similar change in the mode shape of the first global modes. The model variations are summarized in Table 1.

In Table 2, the natural frequencies of the first tower modes are given for all three models. This shows similar natural frequencies for the first tower modes, while the 2nd modes have a variation of about 30 % in the natural frequencies. As the second modes are outside the wave frequency range, this difference is assumed negligible.

Given equal natural periods, the mode shape will determine the sensitivity of each model to wave loads. In Figure 6 the mode shapes of the first and second fore-aft tower modes are shown,

all scaled to give a maximal displacement of 1. As can be seen from the figures, increasing the soil stiffness reduces the displacement in the lower part of the substructure, while the opposite is seen for the model with reduced soil stiffness. It is also worth noticing that the second tower modes show almost no displacement in the tower top for the stiffest soil, which indicates that this mode will not be significantly excited by the thrust force. The excitation due to the rotor tilt moment may still be as significant for this model as for the softer models, as the slope of the modal displacement is approximately equal in all models.

### 3.3. Environmental parameters

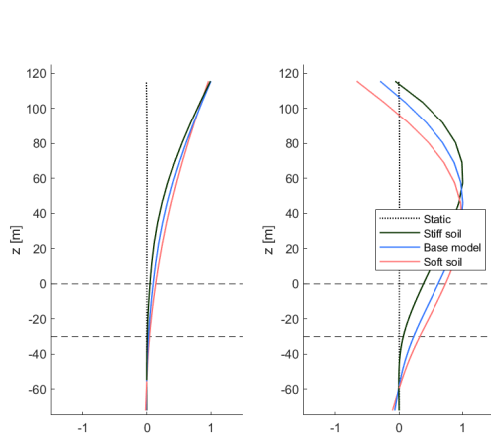


**Figure 6.** 1st (left) and 2nd (right) tower mode in fore-aft direction. The dashed lines show the mean water level and mudline.

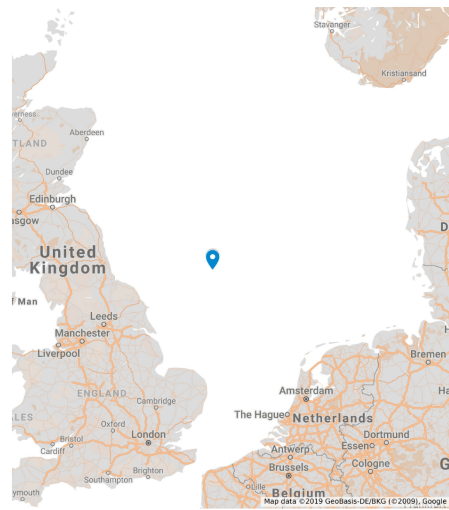


**Figure 7.** Location of metocean data[18].

The environmental conditions are based on 60 years of hindcast data [19], for the location  $54.8^\circ\text{N}$ ,  $1.92^\circ\text{E}$  in Dogger Bank as shown in Figure 7. The joint distribution of wind and waves are described in [18]. In [6], the misalignment between wind and total waves was investigated. Misalignment angles above  $60^\circ$  were found to be rare for significant wave heights above 3 m, while misalignment above  $30^\circ$  is rare for significant wave heights above 5 m. The misalignment bins of  $0^\circ$  and  $30^\circ$  make up more than 75 % of the registered environmental conditions.

Each environmental condition has been simulated as five 1-hour realizations, and the results are based on the average of these realizations. The wind files are generated in TurbSim using the Kaimal wind spectrum and turbulence class B, while the waves are realizations of the JONSWAP spectrum, as defined in [12]. When short-crested waves are simulated, the wave spectrum is modelled as the product of the directional spectrum in Eq. 2 and a JONSWAP spectrum. The spreading parameter  $n$  was set to 2, and the individual wave components are assumed uncoupled. Frequency dependency of the spreading function is not considered.

**3.3.1. Simulation load cases** To reduce the computational effort, the sea states have been lumped to one equivalent sea state per wind speed, as described in [20]. The resulting environmental parameters for aligned wind and waves are shown in Figure 8. Further, it is assumed that the same approach is valid for misaligned wind and waves. The misaligned load cases are found by grouping the absolute value of misalignment to bins of  $30^\circ$ , as shown in Figure 9. One equivalent sea state is found for each wind speed and misalignment bin. A total of 129 load cases are simulated for the misalignment conditions.

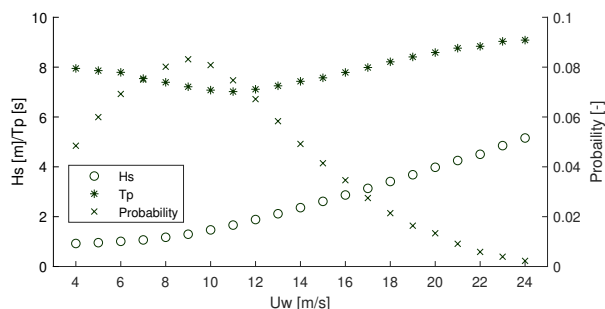


**Figure 8.** Load cases with corresponding probability for aligned wind and waves.

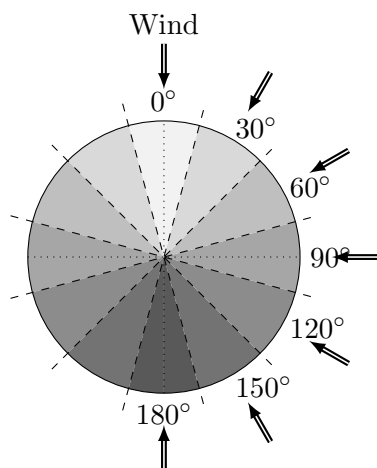


**Figure 9.** Bins for wind/wave misalignment. The wind is always from  $0^\circ$ , while the arrows represent the direction of waves for each bin. Bins with the same absolute value of misalignment, illustrated by the same color, are merged. [6, 21].

### 3.4. Fatigue calculations

The fatigue calculations are performed based on the time series of the axial stress in the monopile and tower, for locations distributed along the length of the support structure. The stress is calculated as

$$\sigma_a(r, \theta) = \frac{N}{A} + \frac{M_y}{I_y} r \cos(\theta) - \frac{M_z}{I_z} r \sin(\theta) \quad (3)$$

where  $N$  is the axial force and  $A$  the cross-section area, while  $r$  is the radius at the calculation point. The bending moments,  $M_y$  and  $M_z$ , second area moments,  $I_y$  and  $I_z$ , and angular position are defined in accordance with the axis system showed in Figure 5.

Knowing the time series of stress, the fatigue damage is calculated using the S-N curve approach and rainflow counting, as implemented in the WAFO package[22] with a correction for a 2-slope S-N curve as given in [23]. The S-N curve for the monopile is assumed to be curve D for steel in sea water with cathodic protection, given in Table 2-2 in [24]. Curve D for steel in air is used for the tower, confer Table 2-1 in [24]. Stress concentration factors due to the presence of e.g. welds should in principle also be considered, but these have been set to 1 for simplicity.

## 4. Results

### 4.1. Aligned wind and waves

The relative importance of the wind and wave loading to the fatigue damage can be found by assuming long-crested waves and aligned wind and waves over the lifetime of the structure. In Figure 10, the relative lifetime contribution to the fatigue damage for each wind speed is shown. The values are normalized by the total fatigue damage for each of the models, so that the figure shows the amount of the total fatigue damage caused by each wind speed.

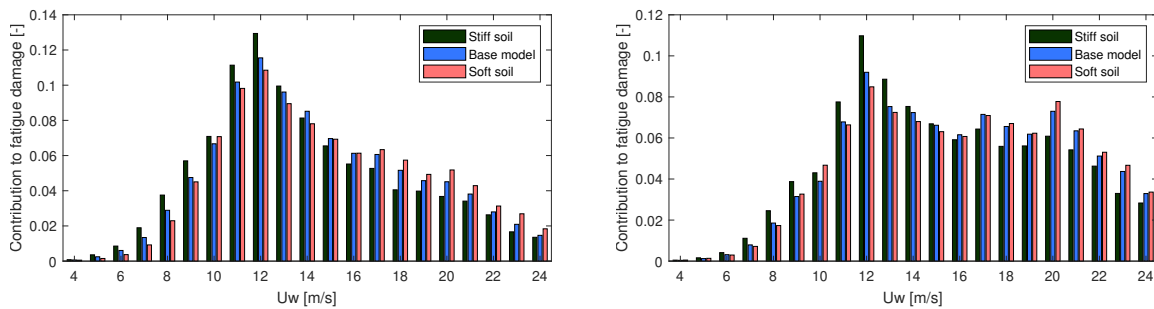


**Figure 10.** Contribution to lifetime fatigue damage per wind speed for the most critical position on tower (left) and monopile (right). The values are normalized by the total fatigue damage for each model.

In the tower, the largest contribution to the fatigue damage is from wind speeds close to rated. These conditions have a high probability of occurrence and are associated with large aerodynamic thrust. In the monopile, the same conditions give the largest contributions to the lifetime fatigue. Still, conditions associated with high wind speeds, corresponding to high waves, show a larger influence on the fatigue damage in the monopile.

The trend is that the model with stiff soil has a larger contribution to the lifetime fatigue damage from conditions where the wind loads are dominating. For the model with soft soil, environmental conditions associated with large wave loads show a larger contribution to the fatigue damage. This indicates that the model with soft soil is more sensitive to wave loads. The effect of modelling the waves as short-crested is expected to be largest for this model, and smallest for the model with stiff soil.

#### 4.2. Wave directionality

When assessing the effect of wave directionality, the wind-wave misalignment and long-term distribution of wind direction is taken into account. The fatigue damage is calculated for various positions around the cross section, and the maximum fatigue damage found for each elevation at the monopile and tower. The ratio  $R_D$  is used to express the effect of short-crested waves:

$$R_D = \frac{D_{SC}(z)}{D_{LC}(z)} \quad (4)$$

where  $D_{SC}(z)$  is the maximum fatigue damage at height  $z$  with short-crested waves.  $D_{LC}(z)$  is the corresponding value with long-crested waves.

Figure 11 shows the distribution of  $R_D$  over the length of the monopile and tower. From the figure, it is seen that the effect on the fatigue damage with short-crested waves is highest on the model with soft soil. This model was also found to be most sensitive to wave loading with aligned wind and waves.

In the monopile, the largest effect of varying the wave directionality model is seen in the upper part of the pile. All models show an increase in fatigue damage for short-crested waves ( $R_D > 1$ ) in the upper part of the pile. The effect is largest for the model with soft soil. This is further explained in Section 4.3.

For the tower, the effect of wave loading is primarily in the tower base, where the response is driven by the aerodynamic thrust and the inertia forces from the rotor-nacelle assembly (RNA). The latter is mainly influenced by the wave loading. Close to the RNA, the response is primarily dominated by the tilting moment of the rotor. The fatigue damage in the tower top is therefore insensitive to the choice of wave model.

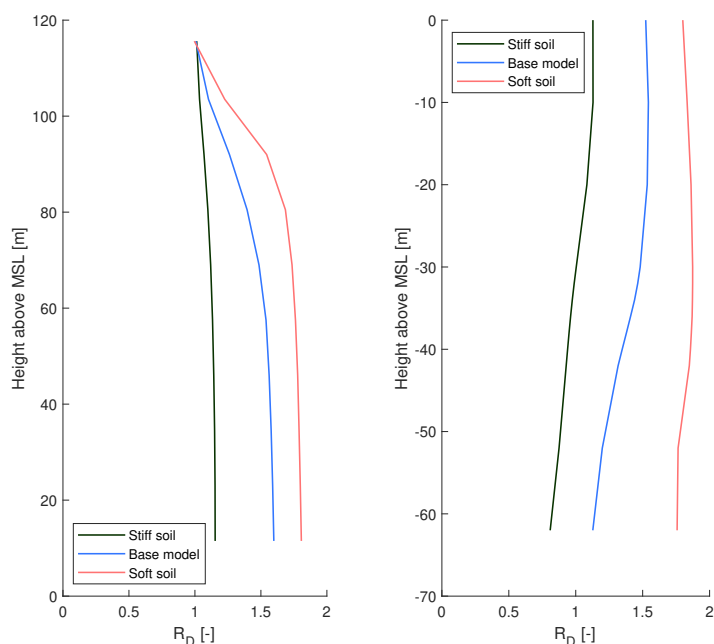


**Figure 11.** Ratio of fatigue damage predicted with short-crested waves to fatigue damage with long-crested waves. Results are shown for the tower (left) and monopile (right).

From a design perspective, it is the highest fatigue damage that is of the most interest. The ratio  $R_D^{max}$  is introduced to describe the influence of wave directionality model on the largest fatigue damage:

$$R_D^{max} = \frac{\max\{D_{SC}(z)\}}{\max\{D_{LC}(z)\}} \quad (5)$$

The values are shown in Figure 12 for both the tower and the pile. For the tower, the values are consistent with the maximum values in Figure 11. This is not the case for the monopile, as the maximum fatigue damage in general occurs for a different depth than the maximum value of  $R_D$ .

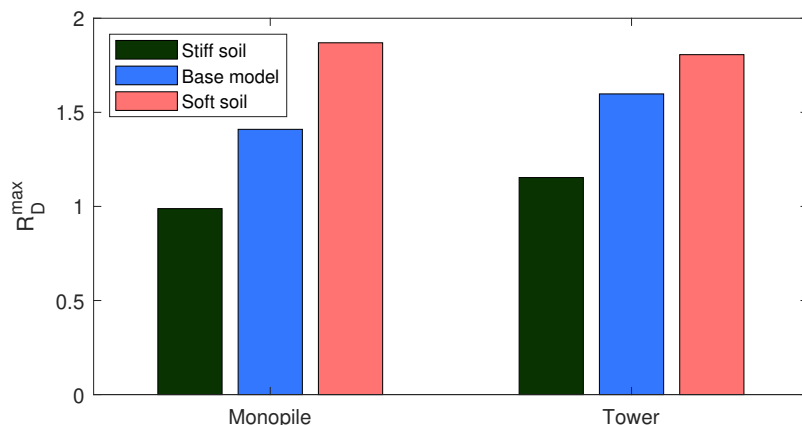


**Figure 12.** Ratio  $R_D^{max}$  for monopile (left) and tower (right)

In summary, long-crested waves only gives a conservative prediction of fatigue damage for the tower with the stiff soil properties. In all other cases, the fatigue damage in the tower and monopile is higher for short-crested waves. This implies that short-crested waves should be considered for fatigue calculations of large monopile foundations.

### 4.3. Selected load cases

While the lifetime fatigue damage at different locations in the support structure is of interest from a design perspective, the long-term distribution of environmental parameters obscures the response under different load conditions. The results from two selected load cases will be given here, for a better understanding of how the response differs when long-crested or short-crested waves is assumed. The key parameters are given in Table 3, and correspond to two of the load cases for wind speed 11 m/s.

**Table 3.** Selected load cases for detailed analysis.

Wind speed [m/s]	$H_s$ [m]	$T_p$ [s]	Misalignment [deg]	Probability of occurrence [-]
11	1.8	5.6	0	4.0 %
11	2	7	60	0.4 %

For the load case with aligned wind and waves, the wave modelling gives small differences in the fore-aft response. This is caused by the high aerodynamic loads and relatively small waves associated with the selected load cases. The response is shown at the left in Figure 13, where the power spectral density (psd) of the fore-aft bending moment at mudline is plotted. The fore-aft response is here defined as the response in the mean wind direction. The difference between the wave models is more significant in the side-side direction. As expected, the side-side response is negligible when long-crested waves is assumed. If short-crested waves is assumed, the peak spectral density is higher than in the fore-aft direction, although the response is very narrow-banded.

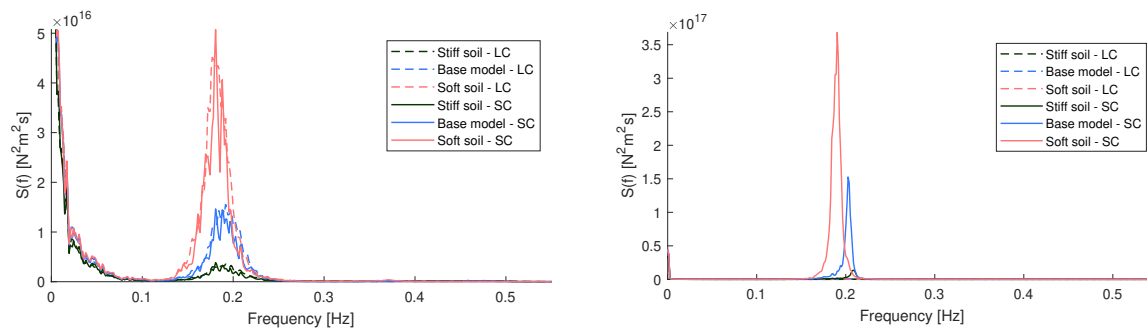


**Figure 13.** Fore-aft (left) and side-side (right) moment spectrum for wind speed 11 m/s and aligned wind and waves

For the misaligned case, the opposite trend is seen. As shown in Figure 14, there is an increase in the fore-aft moment when short-crested waves is assumed. This is as expected from Figure 3, where it is shown that short-crested waves will increase the wave energy in the fore-aft direction for large misalignment angles. The change is most significant for the model with soft soil, and decreases with increasing soil stiffness. In the side-side direction, the change in the response spectrum is now less sensitive to the assumption of long-crested or short-crested waves.

## 5. Discussion

The results show that it can be both conservative and non-conservative to assume long-crested waves in fatigue calculations. While the soil stiffness and tower wall thickness have been altered

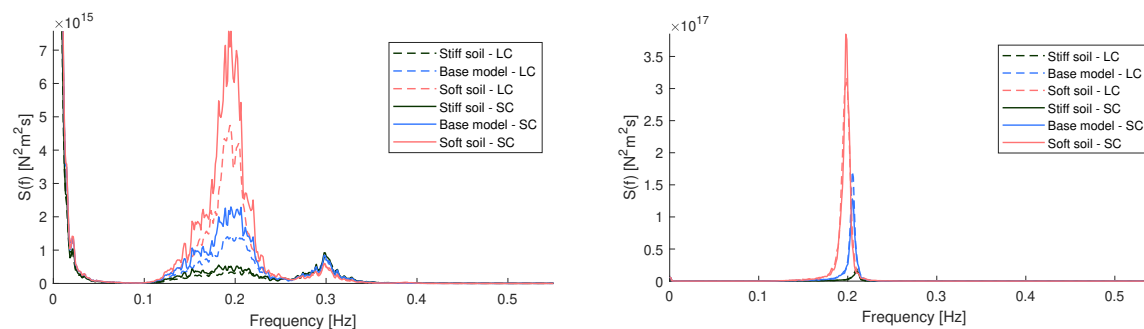


**Figure 14.** Fore-aft (left) and side-side (right) moment spectrum for wind speed 11 m/s and  $60^\circ$  misalignment between wind and waves

here, other parameters may also influence the effect of wave spreading. In general, it can be expected that short-crested waves will yield increased fatigue damage as wave loads become more important. From a design perspective, the mode shape and 1st natural period will influence the structure's sensitivity to waves. A large modal displacement near the mean water level or a natural period close to the wave period will make wave loads more important. This will again make it more important to consider short-crested waves.

The designer can also influence the crosswind damping level, e.g. by fitting tuned mass dampers[25] or applying active load mitigation[2]. Increasing the crosswind damping will reduce the response from waves travelling in the crosswind direction, which can be beneficial when considering both wind-wave misalignment and short-crested waves. Increasing the damping will also make an OWT more similar to the structures analysed by Vugts[8], which will increase the conservatism from assuming long-crested waves.

Several factors that are outside the designer's control will also influence whether it is conservative or not to assume long-crested waves. The effect of short-crested waves depends on the wind-wave misalignment, as shown in Figure 3 and in the selected load cases. If a site evaluated for installation of wind turbines mainly have aligned wind and wave conditions, short-crested waves will increase the fatigue damage. Similarly, short-crested waves at a site with pronounced wind-wave misalignment will reduce the crosswind excitation, potentially reducing the lifetime fatigue damage.

The wave characteristics will also be important in this sense. For the site analysed in this paper, wind-wave misalignment mainly occurs for swell waves. These waves normally have little wave spreading. Thus the fatigue calculations with short-crested swell waves may yield reduced fatigue damage, but the results may be non-conservative since swell waves are mainly long-crested with significant misalignment.

The above discussion shows how complex it is to evaluate whether it is conservative or non-conservative to assume long-crested waves in design calculations. A designer must, therefore, take care to ensure conservative, but not overly conservative, fatigue estimations. Different modelling approaches may be applicable for wave spreading. This will depend on the properties of the support structure, the short-term environmental conditions analysed and the long-term distribution of environmental parameters.

## 6. Conclusion

This paper has investigated the effect of modelling waves as long-crested or short-crested for monopile supported wind turbines in varying soil conditions. Previous studies have concluded that it is conservative to assume long-crested waves in the fatigue calculations of monopile supported OWTs. In this paper, it is shown that this conclusion is not valid for all monopile

designs. As monopile foundations become more sensitive to wave loads, it may be non-conservative to assume long-crested waves. Consequently, short-crested waves should be taken into account when designing monopile foundations for deep water, for soft soil, for harsh wave conditions or with large dimensions.

### Acknowledgments

This work has been carried out at the Centre for Autonomous Marine Operations and Systems (AMOS). The Norwegian Research Council is acknowledged as the main sponsor of NTNU AMOS. This work was supported by the Research Council of Norway through the Centres of Excellence funding scheme, Project number 223254 - AMOS.

### References

- [1] WindEurope 2019 Offshore wind in Europe. Key trends and statistics 2018 Tech. rep.
- [2] Fischer T, de Vries W, Rainey P, Schmidt B, Argyriadis K and Kühn M 2012 **15** 99–117 ISSN 1095-4244
- [3] Fischer T, Rainey P, Bossanyi E and Kühn M 2011 *Wind Engineering* **35** 561–73
- [4] Koukoura C, Brown C, Natarajan A and Vesth A 2016 *Engineering Structures* **120** 147–57
- [5] Kim T and Natarajan A *51st AIAA Aerospace Sciences Meeting including the New Horizons Forum and Aerospace Exposition 2013* (American Institute of Aeronautics and Astronautics Inc.)
- [6] Smilden E, Bachynski E E and Sørensen A J 2017 *ASME 2017 36th International Conference on Ocean, Offshore and Arctic Engineering* (American Society of Mechanical Engineers)
- [7] DNV GL AS 2016 DNVGL-ST-0437 Loads and site conditions for wind turbines
- [8] Vugts J H 2005 *Applied Ocean Research* **27** 173–185 ISSN 0141-1187
- [9] Trumars J M V, Jonsson J O and Bergdahl L 2006 *ASME 2006 25th International Conference on Offshore Mechanics and Arctic Engineering* (ASME)
- [10] Horn J T, Krokstad J R and Amdahl J 2018 *Proceedings of the Institution of Mechanical Engineers, Part M: Journal of Engineering for the Maritime Environment* **232** 37–49
- [11] Arany L, Bhattacharya S, Macdonald J and Hogan S J 2017 *Soil Dynamics and Earthquake Engineering* **92** 126–152 ISSN 0267-7261
- [12] Det Norske Veritas AS 2014 DNV-RP-C205 - Environmental conditions and environmental loads
- [13] Bak C, Zahle F, Bitsche R, Kim T, Yde A, Henriksen L C, Andersen P B, Natarajan A and Hansen M To be accepted *J. Wind Energy*
- [14] Bachynski E E and Ormberg H 2015 *ASME 2015 34th International Conference on Ocean, Offshore and Arctic Engineering* (American Society of Mechanical Engineers)
- [15] The International Organization for Standardization 2016 ISO 19901-4 Geotechnical and foundation design considerations
- [16] Suja-Thauvin L, Krokstad J R and Frimann-Dahl J F 2016 *Energy Procedia* **94** 329–38
- [17] MARINTEK 2015 RIFLEX theory manual
- [18] Horn J T H, Krokstad J R and Amdahl J 2017 Joint probability distribution of environmental conditions for design of offshore wind turbines *ASME 2017 36th International Conference on Ocean, Offshore and Arctic Engineering* (American Society of Mechanical Engineers)
- [19] Reistad M, Breivik O, Haakenstad H, Aarnes O J, Furevik B R and Bidlot J R 2011 *Journal of Geophysical Research: Oceans* **116** 1–18
- [20] Kühn M J 2001 *Dynamics and design optimisation of offshore wind energy conversion systems* Ph.D. thesis TU Delft, Delft University of Technology
- [21] Shrestha B and Kühn M 2016 *Journal of Physics: Conference Series* **753** 1–10
- [22] WAFO-group 2011 *WAFO - A Matlab Toolbox for Analysis of Random Waves and Loads - A Tutorial*
- [23] Bachynski E E, Kvittem M I, Luan C and Moan T 2014 *Journal of Offshore Mechanics and Arctic Engineering* **136** 041902–1–12
- [24] DNV GL AS 2016 DNV-RP-C203 - Fatigue design of offshore steel structures
- [25] Damgaard M, Ibsen L B, Andersen L V and Andersen J K F 2013 *Journal of Wind Engineering and Industrial Aerodynamics* **116** 94–108